Catalytic Oxidation of Volatile Organic Compounds on Manganese and Copper Oxides Supported on Titania

Van Hinh Vu, Jamal Belkouch, Aïssa Ould-Dris, and Bechara Taouk
Laboratoire de Génie des Procédés Industriels, UMR CNRS 6067, Université de Technologie de Compiègne, 60205 Compiègne Cedex, France

DOI 10.1002/aic.11482

A series of mixed oxides supported on TiO_2 ($Mn_{1-y}Cu_yO_x/TiO_2$) synthesized by incipient wetness impregnation method have been characterized and tested for toluene oxidation volatile organic compounds (model). For all catalysts, the total conversion (100%) of toluene into CO_2 was obtained at temperatures higher than 240°C with no catalyst deactivation. At lower temperatures, a gradual deactivation was observed. The most efficient catalyst was $Mn_{0.5}Cu_{0.5}O_x/TiO_2$ (noted $MnCuO_x/T$). Several characterization techniques, XRD, TPR, BET, and TG/DT analysis, were used to explain the catalytic performances. The results allowed attributing the higher activity of $MnCuO_x/T$ to the formation of $Mn_{1.6}Cu_{1.4}O_4$ spinel phase. It has been also demonstrated that the mobility of the catalyst network oxygen is a determining parameter of the catalytic activity. The decrease of activity at a low temperature is related to the adsorption of high molecular weight carbonaceous compounds. However, the catalytic activity is easily regenerated by heating in air flow at 300°C. © 2008 American Institute of Chemical Engineers *AIChE J,* 54: 1585–1591, 2008

Keywords: VOC, toluene, catalytic oxidation, copper-manganese oxides, deactivation

Introduction

The removal of volatile organic compounds (VOC) remains nowadays a challenge for chemists, engineers, and technologists. VOC are considered as air pollutants, because of both directly (toxic or malodorous nature) and indirectly (ozone precursors) harmful effects to human health. Several different techniques have been developed for VOC abatement such as combustion (thermal incineration), absorption, adsorption, and catalytic oxidation. The choice of the technique depends on the VOC concentration and nature as well as the waste gas flow rate.

Catalytic oxidation has been identified as one of the most promising ways to reduce VOC emissions because the reaction temperature is much lower than that required for thermal incineration. The advantage of low oxidation temperature is the reduction of the fuel consumption, particularly for the treatment of large volumes of air containing VOC in low concentrations. Generally, there are two categories of catalysts for VOC abatement: (i) supported noble metals[1,2] and (ii) metal oxides or supported metal oxides.[3–5] Noble metals such as Pt and Pd supported on alumina and silica are well established as efficient catalysts for complete combustion of VOC,[6,7] but they are relatively expensive and their resistance to poisoning is low. Therefore, cheaper catalytic materials, involving transition metal oxides are becoming more attractive. Catalysts based on transition metals (Ni, Cu, Co, Cr, Mn, and Fe) oxides have been intensively studied[8] and the activity shown by these oxides is generally lower than that of noble metal catalysts. However, in particular cases they can be more active than noble metals for VOC destruction.[9] It is therefore evident that, if high activity transition metal-

---

Correspondence concerning this article should be addressed to B. Taouk at bechara.taouk@utc.fr.

based catalysts can be developed for VOC destruction, they will be preferred. As a purpose to combine the advantages of two families of catalysts, many mixtures of noble metals and metal oxides were also studied.[10,11]

Among metal oxide supported catalysts, manganese and copper oxides were considered as the most active for the treatment of CO,[12] NO_x,[13] and VOC.[9] However, one of the most serious problems associated with the commercial application of catalysts for the decomposition of VOC is the catalyst deactivation. As general rule, metal oxide-based catalysts are more poison-tolerant than supported noble metal catalysts.[14] On the other hand, a previous work carried out in our laboratory on the oxidation of toluene[15] and polycyclic hydrocarbons[16] over supported manganese oxide has demonstrated that the catalyst activity increases with the support used in the following order: $MnO_x/SiO_2 < MnO_x/Al_2O_3 < MnO_x/TiO_2$. In addition, Liu et al.[17] have also obtained that titania-supported catalyst gives the highest catalytic activity in total oxidation of chlorinated aromatics in comparison with Al_2O_3 and SiO_2 supports. A systematic investigation of the catalytic activity of different formulations of transition metal oxides (CrOx, MnOx, VOx, SnOx, WOx, NbOx, TaOx, MoOx, ZrOx and BiOx) supported on TiO_2, Al2O3, and SiO_2 catalysts for the total oxidation of benzene showed that for almost all active phases, the conversion increases when the support is changed from SiO_2 to Al2O3 and TiO_2.[18]

In this work, a series of catalysts based on manganese-copper oxide supported on TiO_2 ($Mn_{1-y}Cu_yO_x/TiO_2$) was synthesized by incipient wetness impregnation method, characterized by X-ray diffraction (XRD), temperature programmed reduction (TPR), and TG/DT analysis and tested for the oxidation of toluene as a VOC model. Catalytic performances and catalyst deactivation at low temperature were discussed. Correlations between characterization results and catalytic properties were established.

Experimental

Catalyst preparation

The support used was TiO_2-anatase supplied by Saint-Gobain NorPro with the following properties: pellets of 8 mm height and 3 mm diameter, pore volume of 0.38 $cm^3\ g^{-1}$, and average pore diameter of 15 nm. The TiO_2 pellets were slightly crushed then sieved in order to obtain grains of size ranging between 0.2 and 0.4 mm. The preparations of supported manganese/copper oxides catalysts were carried out by the incipient wetness impregnation method. The mixed aqueous solution of manganese nitrate ($Mn(NO_3)_2 \cdot 4H_2O$) and/or copper nitrate ($Cu(NO_3)_2 \cdot 3H_2O$) was added drop wise into a beaker containing the grains of TiO_2. The impregnated samples were dried at 100°C for 5 h and finally calcined at 500°C for 7 h in air.

The general formula of the prepared catalysts was $Mn_{1-y}Cu_yO_x/TiO_2$. The ratio of metal (Mn and/or Cu) loading of supported oxides on titania is 5 wt % based on the amount of precursor salts. Samples with the following molar ratios of Mn/Cu were prepared: Mn/Cu = 1/0 ($y = 0$); 3/1 ($y = 0.25$); 2/1 ($y = 0.33$); 1/1 ($y = 0.5$); 1/2 ($y = 0.66$); 1/3 ($y = 0.75$), and 0/1 ($y = 1$). The obtained samples were noted: MnO_x/T, Mn_3CuO_x/T, Mn_2CuO_x/T, $MnCuO_x/T$, $MnCu_2O_x/T$, $MnCu_3O_x/T$, and CuO_x/T, respectively, with $T = TiO_2$.

Catalyst characterization

For a better understanding of catalysts behavior, the characterization by XRD, TPR, BET measurement of specific surface area and TG/DT analysis were performed.

The BET specific surface area of the catalysts was determined in a conventional static volume apparatus (Micromeritics ASAP 2020) operating with N_2 adsorption at −196°C. The samples were first degassed during 3 h at 300°C in a pure nitrogen flow.

The patterns of XRD ($2\theta = 5°–125°$) of catalysts powders were obtained using a diffractometer (Inel cps 120) equipped with an iron anticathode ($\lambda = 1.936$ E) and an ethane ionization curved detector.

The differential thermal analysis (DTA) and thermogravimetric analysis (TGA) were carried out simultaneously using Setaram TG 92 apparatus. During the experiments a flow of 1.2 L h^{-1} of air or nitrogen was passed over the catalyst and the temperature was increased from room temperature to 800°C with a heating rate of 10°C min^{-1}.

The TPR experiments were performed in a mixture of 5 vol % of hydrogen in nitrogen with a flow rate of 20 $cm^3\ min^{-1}$. The temperature of sample was varied from room temperature to 800°C with a heating rate of 10°C min^{-1}. The hydrogen consumption was measured using a thermal conductivity detector.

Catalytic tests

Catalytic tests were carried out in a fixed-bed reactor (height = 60 cm, i.d. = 2.7 cm) at atmospheric pressure and in the temperature range of 150–300°C during at least 5 h. The bench test is shown in Figure 1. The volume of catalytic bed was 10 cm^3. The air flow rate was 50 L h^{-1} corresponding to the Gas Hourly Space Velocity (GHSV) of 5000 h^{-1}. Toluene was fed to the reactor by means of a saturator where a part of the air is introduced at a controlled temperature. The concentration of toluene in air was about 500 ppm (3500 ppm equiv. CH_4). The feed and the reactor outflow gases were analyzed on-line by various analyzers: toluene by FID analyzer (Environment SA—Graphite 52M), CO and CO_2 by IR absorption (Leybold BINOS 1001), and O_2 by

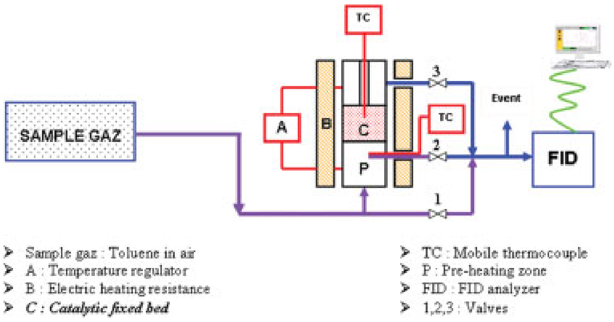

Figure 1. Scheme of the fixed bed reactor and the catalytic test outline.

[Color figure can be viewed in the online issue, which is available at www.interscience.wiley.com.]

Table 1. Crystalline Phases, Specific Surface Areas, and H_2 Consumption Measured by TPR for the Prepared Catalysts

Formula	XRD-Identified Phases	BET Surface (m^2 g^{-1})	H_2 Consumption (mol g^{-1})
TiO_2*	Anatase TiO_2 (T)	49	1.63×10^{-4}
MnO_x/T	Mn_2O_3[†] + T	57	7.16×10^{-4}
Mn_3CuO_x/T	Mn_2O_3[†] + $Mn_{1.6}Cu_{1.4}O_4$ + T	48	1.01×10^{-3}
Mn_2CuO_x/T	Mn_2O_3[†] + $Mn_{1.6}Cu_{1.4}O_4$ + T	40	1.00×10^{-3}
$MnCuO_x$/T	Mn_2O_3[†] + $Mn_{1.6}Cu_{1.4}O_4$ + CuO[‡]+ T	41	1.06×10^{-3}
$MnCu_2O_x$/T	$Mn_{1.6}Cu_{1.4}O_4$ + CuO[‡]+ T	34	9.64×10^{-4}
$MnCu_3O_x$/T	$Mn_{1.6}Cu_{1.4}O_4$ + CuO[‡]+ T	37	9.93×10^{-4}
CuO_x/T	CuO[‡] + T	26	9.74×10^{-4}

*Commercial product.
[†]Bixbyite—Mn_2O_3.
[‡]Tenorite—CuO.

paramagnetism (Leybold OXYNOS 100). FID analyzer was previously calibrated using three concentrations of propane calibrating gas (915, 788, and 80.3 ppm ± 2%). CO, CO_2, and O_2 analyzers were calibrated with a gas having the composition (CO_2:782 ppm, CO = 97.7 ppm, O_2:14.89 molar % and the balance of N_2 ± 2%).

Before each a series of tests, a blank test was carried out with pure SiO_2 as an inert material and resulted in no conversion of toluene.

The conversion of toluene was calculated from the amount of toluene in the inlet and outlet of the reactor ($[\text{toluene}]_{in} - [\text{toluene}]_{out})/[\text{toluene}]_{in}$). After each test, the regeneration of catalysts was carried out in flowing air for the same GHSV (5000 h^{-1}) at 300°C during 2 h.

Results and Discussions

Characterization results

The specific surface areas and the crystalline phases clearly identified by XRD for all catalysts studied are summarized in Table 1.

All catalysts show a specific surface area lower than non impregnated support except MnO_x/T. This surface decreases with the increase of copper content (Cu/Mn ratio), it passes from 57 m^2 g^{-1} for MnO_x/T to 26 m^2 g^{-1} for the CuO_x/T sample. This result is in good agreement with previous works.[8,16] García[8] reported that MnO_x catalyst (76 m^2 g^{-1}) had a specific surface area greater than CuO_x (20 m^2 g^{-1}) and the study of Andersson and Larsson[16] showed that the increase of Cu content on alumina decreased its surface area.

In the case of XRD characterization, the metal content 5 wt % (Mn + Cu) was not enough to identify the phases formed on TiO_2 surface. Therefore a series of samples with 20 wt % (Mn + Cu) were prepared with respect to the same formulations than that of 5 wt % series. The XRD patterns of TiO_2 (T), MnO_x/T, CuO_x/T, and $Mn_{1-y}Cu_yO_x$/T catalysts are shown in Figure 2. The XRD pattern of the support displays the anatase phase which was also detected in all other catalysts. This result demonstrates that the support was not transformed. For the MnO_x/T catalyst, only Mn_2O_3 was detected with a characteristic peak at 2θ = 41.7°. The same peak is observed for Mn-Cu mixed samples with a diminu-

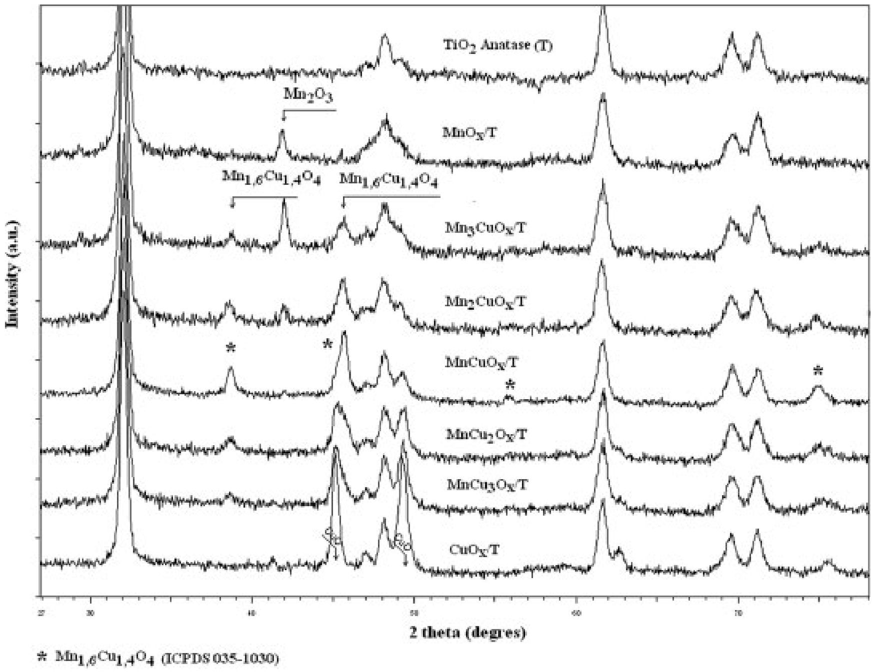

Figure 2. XRD patterns of $Mn_{1-y}Cu_yO_x$/T catalyst combinations.

tion of intensity when Mn content decreases. The same result was obtained by Liu et al.[17] who reported that the XRD peaks of Mn_2O_3 are detected when Mn loading (on TiO_2) after the calcination at 500°C is 6.3 wt %.

CuO_x/T catalyst exhibits three strong CuO characteristic peaks at $2\theta = 45$; 49.5 and 62.5. Two other smaller peaks are observed at $2\theta = 41$ and 75.5. The intensities of these peaks decrease when Cu content decreases in Mn-Cu combinations.

In addition to CuO and Mn_2O_3 phases, a mixed spinel type oxide $Mn_{1.6}Cu_{1.4}O_4$ was also identified (ICPDS 035-1030). The characteristic peaks of this phase at $2\theta = 38.5$, 45.5, 55.5, and 74.5 corresponding to the reticular planes (220), (311), (511), and (440), respectively, are observed in all cases where Cu and Mn are simultaneously present. The intensities of these peaks vary with the Mn/Cu ratio and reach a maximum for $MnCuO_x/T$ catalyst. This result indicates that the Mn/Cu ratio = 1 is the most favourable ratio for the formation of $Mn_{1.6}Cu_{1.4}O_4$ phase. This phase is very close to $CuMn_2O_4$ hopcalite which has spinel crystalline structure, a well-known catalyst for the oxidation of CO into CO_2.[12,19] The $Cu_{1.4}Mn_{1.6}O_4$ formula can be written as $Cu_{1+\alpha}Mn_{2-\alpha}O_4$ with $\alpha = 0.4$.

Catalytic performances

As indicated above, gases at the inlet and outlet of the reactor were continuously analyzed by FID analyzer to determine the toluene conversion as a function of time, at a given temperature. To confirm the catalytic activity, a test has been previously carried out with pure SiO_2 as an inert material and resulted in no conversion of toluene at temperatures up to 240°C. Generally, all the catalysts tested reveal a high activity for the total oxidation of toluene. For all Mn-Cu combinations, toluene is completely converted exclusively into CO_2 when the temperature exceeds 260°C. However, at a temperature lower than 240°C, the conversion inevitably decreases with time. For example, Figure 3 shows the conversion vs. time at 250 and 230°C for $CuMnO_x/T$ catalyst. At 250°C, the conversion of toluene was maintained at 100% during 14 h while at 230°C, some deactivation was observed. As it can be observed in Figure 4, this deactivation is more important when the temperature is lower: the conversion reaches 100% at 250°C and remains stable while at 200°C it falls to 48% and to 21% after 1 and 4 h, respectively.

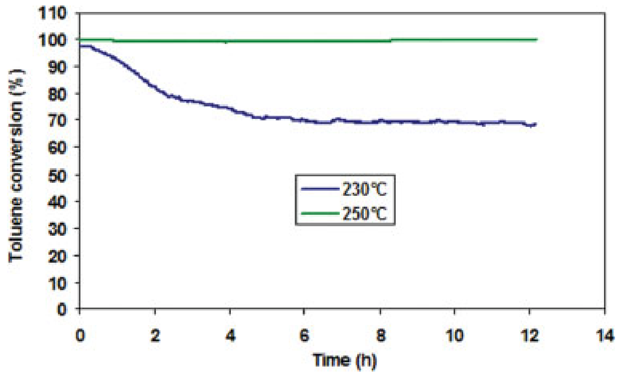

Figure 3. Toluene conversion vs. time for $MnCuO_x/T$ catalyst at 230 and 250°C.

[Color figure can be viewed in the online issue, which is available at www.interscience.wiley.com.]

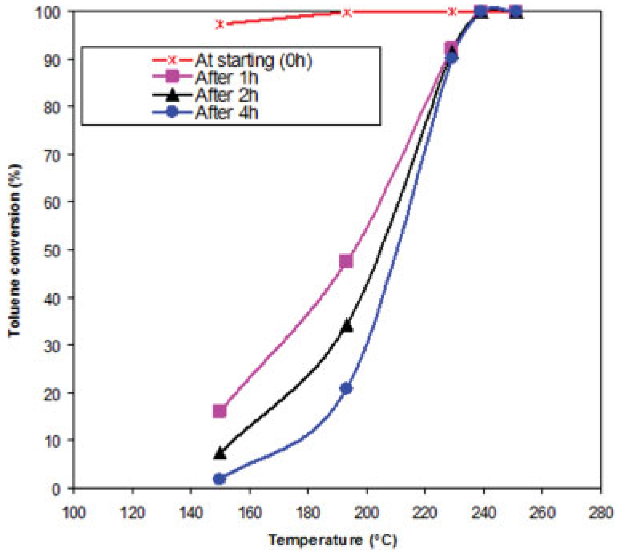

Figure 4. Toluene conversion for $MnCuO_x/T$ as a function of temperature at different running times.

[Color figure can be viewed in the online issue, which is available at www.interscience.wiley.com.]

To compare the different catalysts prepared, the tests were carried out at a temperature lower than 240°C so a difference in the toluene conversion could be observed. The results of toluene conversion with time at 230°C with the different catalysts tested are presented in Figure 5. It can be seen that the apparent conversion, close to 100% at the beginning of the test for all catalysts, progressively decreases with the duration of the test. The toluene conversion which decreases more or less quickly according to the catalyst tested is the consequence of the catalyst deactivation. The catalysts are compared according to the conversion obtained at a given running time. Hence, it can be noted that:

(i) CuO_x/T is more active than MnO_x/T;

(ii) all Mn-Cu combination catalysts supported on titania were more active than MnO_x/T;

(iii) the optimal catalytic activity is obtained with $MnCuO_x/T$ (Mn/Cu = 1).

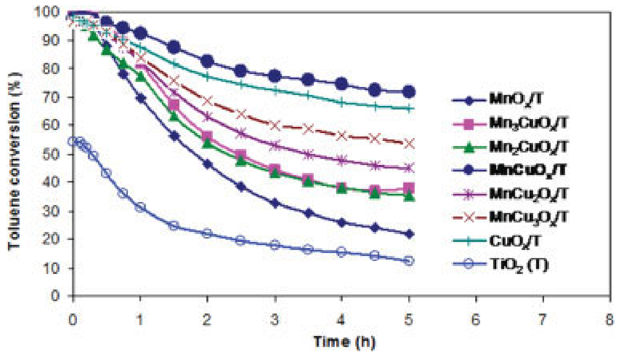

Figure 5. Toluene conversion for $Mn_{1-y}Cu_yO_x/T$ catalyst combinations at 230°C vs. time.

[Color figure can be viewed in the online issue, which is available at www.interscience.wiley.com.]

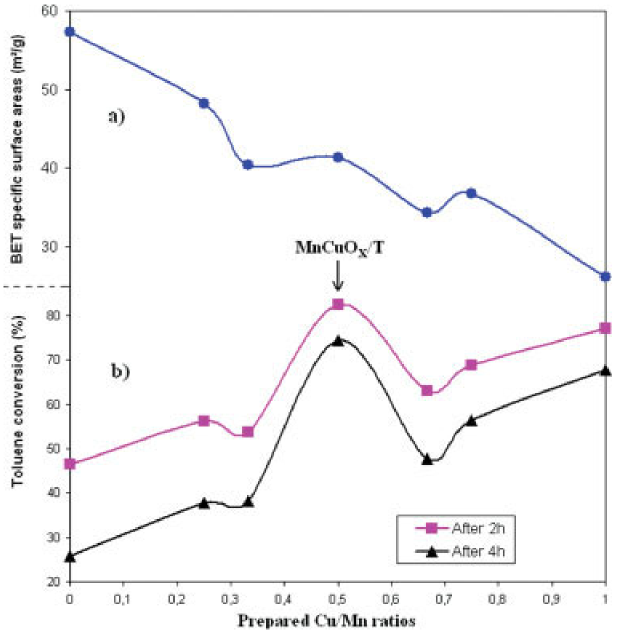

Figure 6. (a) BET specific surface area and (b) toluene conversion at different moments of time during the catalytic tests as a function of Cu/Mn molar ratio for $Mn_{1-y}Cu_yO_x$/T catalyst combinations.

[Color figure can be viewed in the online issue, which is available at www.interscience.wiley.com.]

For a better understanding of the catalytic activity evolution, the variations of toluene conversion and specific surface area with the Cu/Mn ratio are presented in Figure 6. The general tendency is that the activity increases with the Cu/Mn ratio whereas the specific surface area decreases. The optimal activity was obtained for MnCuO$_x$/T. The activity of the catalysts could be classified as follows:

$$\mathrm{T} \ll \mathrm{MnO}_x/\mathrm{T} < \mathrm{Mn_2CuO}_x/\mathrm{T} \approx \mathrm{Mn_3CuO}_x/\mathrm{T}$$
$$< \mathrm{MnCu_2O}_x/\mathrm{T} < \mathrm{MnCu_3O}_x/\mathrm{T} < \mathrm{CuO}_x/\mathrm{T} < \mathrm{MnCuO}_x/\mathrm{T}.$$

A global observation of these results indicates that the specific surface area is not the principal parameter which is influencing the catalytic activity. On the other hand, the XRD results (Figure 2) are able to connect the particularly high activity of the CuMnO$_x$/T to the presence of the $Mn_{1.6}Cu_{1.4}O_4$ spinel phase in greater proportion.

Deactivation and regeneration of catalysts

To examine the reversibility of the catalyst deactivation, treatments of used catalysts under air flow at 300°C were carried out. The catalytic activity was entirely recovered for all samples confirming that the catalyst regeneration is complete. The strong adsorption of toluene and other high molecular weight carbonaceous compounds and even a coke formation on the catalysts surface could be the mechanism causing the catalyst deactivation. To elucidate this question, TG-DTA of the fresh and used MnCuO$_x$/T catalysts were performed under both air and nitrogen atmosphere. The results of this analysis are presented in Figure 7.

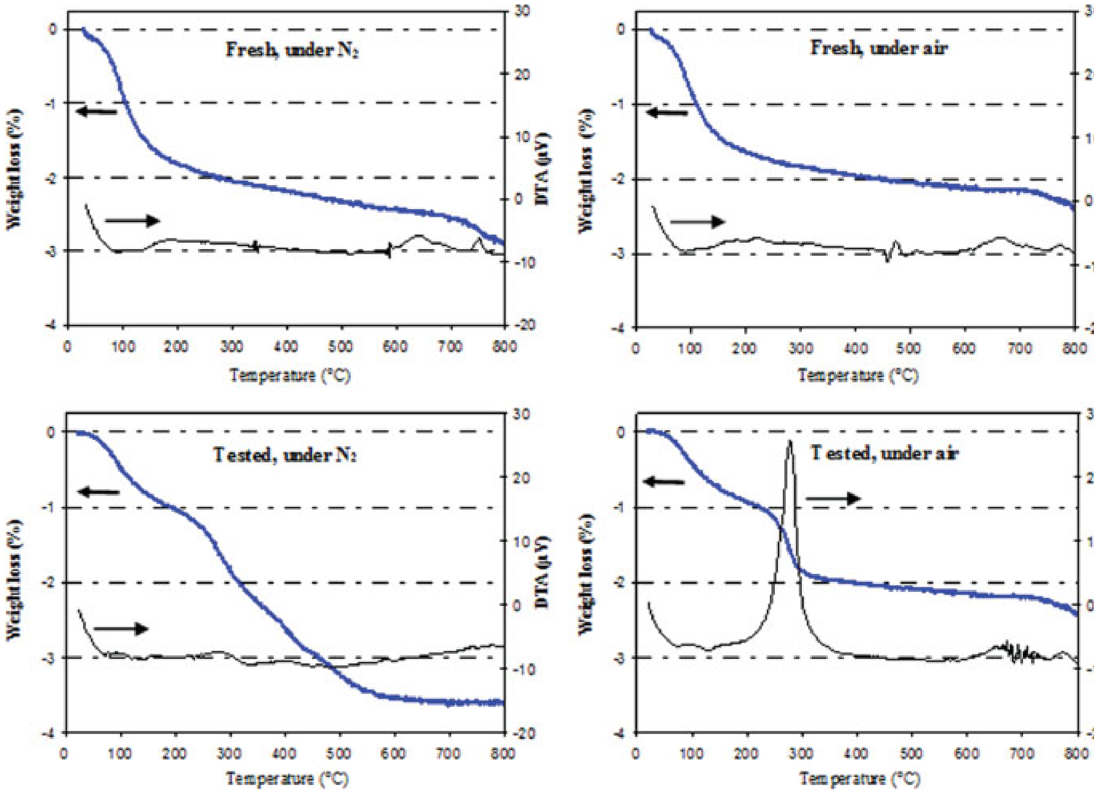

Figure 7. TG-DTA curves of fresh and used MnCuOx/T catalyst under air and nitrogen.

[Color figure can be viewed in the online issue, which is available at www.interscience.wiley.com.]

The TGA curve under air of a previously tested catalyst for toluene oxidation presents two principal weight losses. The first (~0.9%) which is around 100°C should correspond to the water loss. The second weight loss (~1%) is observed around 280°C. The related DTA curve (presented in the same figure) shows the strongly exothermic character which is able to ascribe without ambiguity this weight loss to the combustion of the accumulated high molecular weight carbonaceous compounds or coke deposit on the catalyst surface. This result is also capable to explain why at a temperature higher than 260°C, catalysts deactivation was not observed and why their regeneration during 2 h under air at about 300°C, recovered entirely the initial activity of catalysts.

The TG-DTA curves under nitrogen of the same sample show in evidence, a global weight loss that is slower, but more important and more complex than that observed under air. We can reasonably discriminate the first loss observed at around 100°C corresponding to the water desorption from the second which is spread out from 200°C until 600°C. The low intensity of the obtained DTA peaks makes the interpretation difficult. Although the analysis was carried out under inert gas (nitrogen), the second weight loss is greater than that one obtained under air flow (~2% instead of 1%). This phenomenon can be explained by the fact that the oxidation of the coke deposit on catalyst surface took place with the contribution of oxygen of the catalyst network. The global weight is thus equal to the sum of the mass of oxidized coke deposit and oxygen mass of the catalyst network used for this oxidation.

The oxygen contribution from catalyst network indicates an oxidation according to Mars-Van Krevelen redox mechanism[20] that is well known in the catalytic oxidation by oxide catalysts. This mechanism includes two steps: the first step consists of the reactant oxidation using the catalyst network oxygen which will be replaced, in the second step by gaseous oxygen. In the case of TG-DTA under nitrogen flow, the oxygen of catalyst could not be replaced and a consequent additional weight loss was observed.

The analysis of fresh catalyst (before test, Figure 7) gave practically the same curves under both air and nitrogen atmospheres. Only the water weight loss at around 100°C is observed. The absence of other losses in this case confirms that the losses detected for the used catalyst are due to the coke deposit during the test which is responsible of the catalyst deactivation.

Reductibility of catalysts, TPR characterization

As aforementioned, toluene oxidation mechanism on studied catalysts is certainly the redox type in which Cu and/or Mn change continuously and reversibly their oxidation state. At the same time, the oxygen of the catalyst network contributes to the oxidation reaction. The mobility of this oxygen is of a great importance and the TPR study of the catalysts can shed light on such mobility.

The TPR results for all samples tested including pure TiO_2 are presented in Figure 8 and the amount H_2 consumption (mol/g of catalyst) is given in Table 1. The TPR curve of CuO_x/T presents three peaks (at 261°C, 305°C, and ~440°C). The XRD characterization revealed that CuO phase is present in this catalyst (Figure 2). Generally, the bulk CuO reduction under hydrogen leads to copper metal according to $CuO \rightarrow Cu_2O \rightarrow Cu$ sequence and results in only one TPR peak at around 450°C. However, in the case of supported CuO (CuO_x/T), two peaks (both corresponding to the same sequence) are observed[21,22]: the first is ascribed to CuO which is in strong interaction with the support by forming superficial monolayer and the second corresponds to another part of CuO species having a weak interaction with TiO_2. In our case, these two peaks were observed at 261 and 305°C, respectively. The third peak observed around 440°C can be ascribed to a superficial reduction of TiO_2. Indeed, this peak was also observed by Wöllner[21] and was attributed to a weak reduction of TiO_2. The TiO_2 support alone presents only one weak reduction at about 640°C (Figure 8). When TiO_2 is used as support for active phase containing copper oxide, it is partially reduced at a lower temperature due to the catalytic effect (on TiO_2 reduction) of formed Cu^0 during the CuO reduction.

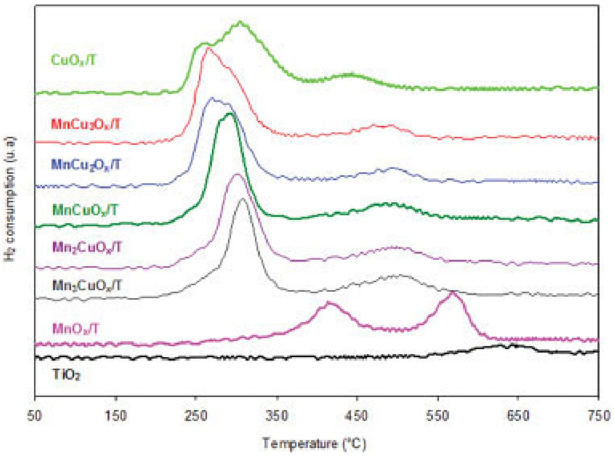

Figure 8. TPR curves of TiO_2 support and all catalysts tested.

[Color figure can be viewed in the online issue, which is available at www.interscience.wiley.com.]

In the case of MnO_x/T, two reduction peaks are observed at 417 and 568°C. According to XRD analysis, the manganese oxide in this case is Mn_2O_3. The two peaks are associated with the following reduction states: $Mn_2O_3 \rightarrow Mn_3O_4$ and $Mn_3O_4 \rightarrow MnO$, respectively.[23]

TPR curves of all $Mn_{1-y}Cu_yO_x$/T are similar and are characterized by the presence of two peaks. The first peak which is attributed to the simultaneous reduction of Cu and Mn oxides is located around 268°C for $MnCu_3O_x$/T and moves towards high temperatures when the Mn/Cu ratio increases. The temperature of this first peak is 292°C for $MnCuO_x$/T catalyst and 310°C for Mn_3CuO_x/T. The second peak is relatively broad and not very intense. Its position is around 490°C and its intensity is very slightly affected by the Mn/Cu ratio. As for CuO_x/T, this peak is ascribed to the partial reduction of TiO_2 with a slight displacement towards high temperatures caused by the increase of the manganese content (decrease of Cu/Mn ratio). The comparison of the curves of all $Mn_{1-y}Cu_yO_x$/T samples with those of CuO_x/T and MnO_x/T indicates that copper and manganese are reduced at the same time at an intermediate temperature between those of CuO and Mn_2O_3 reductions. This phenomenon is in agreement with the work of Hahn and coworkers[12] who studied the $CuMn_2O_4$ spinel as a bulk catalyst for CO oxidation. It should be noted that, in all cases, the reduction temperature of the phases supported on TiO_2 is lower than that of non supported corresponding phases (bulk oxides). The reduction is supported by the presence of the TiO_2, the formation of the spinel phase and the close contact between various oxide phases when they coexist. The fact that the reduction is easier in the case of the Cu-Mn/TiO_2 combinations demonstrates that there is an increase of the catalyst network oxygen mobility and consequently an improvement of the catalytic activity.

Conclusions

This study showed that the manganese/copper oxides catalysts supported on TiO_2 anatase are very active for toluene oxidation used as a VOC model. At a temperature higher than 260°C, all the Mn-Cu combinations supported on TiO_2 resulted in a total conversion of the toluene into CO_2 and no catalyst deactivation was observed. The catalytic activity has been found to vary with the Mn/Cu ratio. Among the series tested, $CuMnO_x$/T catalyst (Mn/Cu = 1) has given the best result, demonstrated by a total toluene conversion at 240°C. The characterization of the tested catalysts was capable to attribute the optimization of the catalytic activity to the formation of the $Mn_{1.6}Cu_{1.4}O_4$ spinel phase.

At temperatures lower than 240°C, a progressive deactivation of the catalyst was observed. It is due to a strong adsorption of carbonaceous species and/or coke formation on the catalyst surface. The regeneration in air at about 300°C enables the catalyst to recover all of its initial activity. This deactivation is thus perfectly reversible.

The TGA-DTA characterization of all catalysts was able to support the hypothesis of a redox reaction mechanism that involves the oxide catalysts network oxygen. The TPR results showed that the mobility of network oxygen is improved by the presence of the support (TiO_2) and by the combination of manganese and copper oxides.

Literature Cited

1. Wu JCS, Chang TY. VOC deep oxidation over Pt catalysts using hydrophobic supports. *Catal Today*. 1998;44:111–118.
2. Luo MF, He M, Xie YL, Fang P, Jin LY. Toluene oxidation on Pd catalysts supported by CeO_2-Y_2O_3 washcoated cordierite honeycomb. *Appl Catal B*. 2007;69:213–218.
3. Alifanti M, Florea M, Somacescu S, Parvulescu VI. Supported perovskites for total oxidation of toluene. *Appl Catal B*. 2005;60:33–39.
4. Blasin-Aubé V, Belkouch J, Monceaux L. General study of catalytic oxidation of various VOCs over $La_{0,8}Sr_{0,2}MnO_{3+x}$ perovskite catalyst—influence of mixture. *Appl Catal B*. 2003;43:175–186.
5. Haihal I, Belkouch J, Taouk B. *Récents Progrès en Génie des Procédés, Numéro 92, 2005. ISBN 2–910239-66–7, Ed.* SFGP, Paris, France.
6. Tsou J, Pinard L, Magnoux P, Figueiredo JL, Guisnet M. Catalytic oxidation of volatile organic compounds (VOCs). Oxidation of o-xylene over Pt/HBEA catalysts. *Appl Catal B*. 2003;46:371–379.
7. Hori K, Matsune H, Takenaka S, Kishida M. Preparation of silica-coated Pt metal nanoparticles using microemulsion and their catalytic performance. *Sci Technol Adv Mater*. 2006;7:678–684.
8. García T, Solsona B, Taylor SH. Naphthalene total oxidation over metal oxide catalysts. *Appl Catal B*. 2006;66:92–99.
9. Lahousse C, Bernier A, Grange P, Delmon B, Papaefthimiou P, Ioannides T, Verykiosy X. Evaluation of γ-MnO_2 as a VOC removal catalyst: comparison with a noble metal catalyst. *J Catal*. 1998; 178:214–225.
10. Tidahy HL, Siffert S, Wyrwalski F, Lamonier JF, Aboukaïs A. Catalytic activity of copper and palladium based catalysts for toluene total oxidation. *Catal Today*. 2007;119:317–320.
11. O'shea VAP, Álvarez-Galván MC, Fierro JLG, Arias PL. Influence of feed composition on the activity of Mn and PdMn/Al_2O_3 catalysts for combustion of formaldehyde/methanol. *Appl Catal B*. 2005;57: 191–199.
12. Buciuman FC, Patcas F, Hahn T. A spillover approach to oxidation catalysis over copper and manganese mixed oxides. *Chem Eng Proc*. 1999;38:563–569.
13. Kang M, Park ED, Kim JM, Yie JE. Cu-Mn mixed oxides for low temperature NO reduction with NH_3. *Catal Today*. 2006;111:236–241.
14. Spivey JJ, Butt JB. Literature review: deactivation of catalysts in the oxidation of volatile organic compounds. *Catal Today*. 1992;11:465–590.
15. Haihal I. Dépollution catalytique des effluents gazeux contenant des hydrocarbures aromatiques par des catalyseurs à base d'oxydes de manganèse. PhD Thesis, Université de Technologie de Compiègne: France, 2004.
16. Larsson PO, Andersson A. Oxides of copper, ceria promoted copper, manganese and copper manganese on Al_2O_3 for the combustion of CO, ethyl acetate and ethanol. *Appl Catal B*. 2000;24:175–192.
17. Liu Y, Luo M, Wei Z, Xin Q, Ying P, Li C. Catalytic oxidation of chlorobenzene on supported manganese oxide catalysts. *Appl Catal B*. 2001;29:61–67.
18. Bertinchamps F, Grégoire C, Gaigneaux EM. Systematic investigation of supported transition metal oxide based formulations for the catalytic oxidative elimination of (chloro)-aromatics. *Appl Catal B*. 2006;66:1–9.
19. Krämer M, Schmidt T, Stöwe K, Maier WF. Structural and catalytic aspects of sol-gel derived copper manganese oxides as low-temperature CO oxidation catalyst. *Appl Catal A*. 2006;302:257–263.
20. Doornkamp C, Ponec V. The universal character of the Mars and Van Krevelen mechanism. *J Mol Catal A: Chem*. 2000;162:19–32.
21. Wöllner A, Lange F, Schmelz H, Knözinger H. Characterization of mixed copper-manganese oxides supported on titania catalysts for selective oxidation of ammonia. *Appl Catal A*. 1993;94:181–203.
22. Larsson PO, Andersson A, Wallenberg LR, Svensson B. Combustion of CO and Toluene; characterisation of copper oxide supported on titania and activity comparisons with supported cobalt, iron, and manganese oxide. *J Catal*. 1996;163:279–293.
23. Kapteijn F, Singoredjo L, Andreini A, Moulijn JA. Activity and selectivity of pure manganese oxides in the selective catalytic reduction of nitric oxide with ammonia. *Appl Catal B*. 1994;3:173–189.

Manuscript received Oct. 8, 2007, and revision received Feb. 11, 2008.